Effect of Relative Humidity on the Composition of Secondary Organic Aerosol from Oxidation of Toluene

Mallory L. Hinks,[1] Julia Montoya-Aguilera,[1] Lucas Ellison,[1] Peng Lin,[2] Alexander Laskin,[2] Julia Laskin,[2] Manabu Shiraiwa,[1] Donald Dabdub,[3] and Sergey A. Nizkorodov[1]

[1]Department of Chemistry, University of California Irvine, Irvine, CA 92697
[2]Department of Chemistry, Purdue University, West Lafayette, IN 47907, USA
[3]Department of Mechanical and Aerospace Engineering, University of California Irvine, Irvine, CA 92697

Correspondence to: Sergey A. Nizkorodov (nizkorod@uci.edu)

Abstract. The effect of relative humidity (RH) on the chemical composition of secondary organic aerosol (SOA) formed from low-NO_x toluene oxidation was investigated. SOA samples were prepared in an aerosol smog chamber at <2% RH and 75% RH, collected on Teflon filters and analyzed with nanospray desorption electrospray ionization high-resolution mass spectrometry (nano-DESI-HRMS). Measurements revealed a significant reduction in the fraction of oligomers present in the SOA generated at 75% RH compared to SOA generated under dry conditions. In a separate set of experiments, the particle mass concentrations were measured with a Scanning Mobility Particle Sizer (SMPS) at RHs ranging from <2% to 90%. It was found that the particle mass loading decreased by nearly an order of magnitude when RH increased from <2% to 75-90% for low-NO_x toluene SOA. The volatility distributions of the SOA compounds, estimated from the distribution of molecular formulas using the "molecular corridor" approach, confirmed that SOA became more volatile on average under high RH conditions. In contrast, the effect of RH on SOA mass loading was found to be much smaller for high-NO_x toluene SOA. The observed increase in the oligomer fraction and particle mass loading were attributed to enhancement of condensation reactions under dry conditions.

1 Introduction

Secondary organic aerosol (SOA) is an important component of atmospheric particulate matter. It is formed in the atmosphere via oxidation of volatile organic compounds (VOCs) by common atmospheric oxidants such as O_3, OH, and NO_3 (Seinfeld and Pandis, 2016). The SOA formation mechanisms depend in a complex way on environmental parameters such as solar irradiance, temperature, and relative humidity (RH). The RH controls the amount of available water, and therefore affects processes in which water acts as a reactant, product, or solvent in several ways. Firstly, gaseous water can directly participate in the VOC oxidation reactions. For example, it is well known to react with carbonyl oxide intermediates in

ozonolysis of alkenes (Finlayson-Pitts and Pitts Jr, 2000). Additionally, aerosol liquid water present in hygroscopic particles can lead to hydrolysis of organic compounds and other particle-phase reactions involving or catalyzed by water (Ervens et al., 2011). Aerosol liquid water also has a strong effect on acidity of particles and, therefore, affects acid-catalyzed processes occurring in particles (Jang et al., 2002). Furthermore, water can act as a plasticizer for SOA particles making them less

5 viscous, thus affecting the rate of their growth (Renbaum-Wolff et al., 2013; Perraud et al., 2012; Shiraiwa and Seinfeld, 2012). Under supersaturated conditions, aqueous chemistry occurring in cloud and fog droplets promotes conversion of small water-soluble molecules into non-volatile products that would not form in the absence of liquid water (Herrmann et al., 2015). Finally, water also promotes photodegradation of dissolved SOA compounds (Bateman et al., 2011; Nguyen et al., 2012; Romonosky et al., 2015; Romonosky et al., 2017).

10 Chemical composition is an important characteristic of SOA because it determines the climate and health relevant properties. The effect of RH on the chemical composition of SOA has been studied for several types of SOA (Nguyen et al., 2011; Zhang et al., 2011; Riva et al., 2016; Harvey et al., 2016). For example, Nguyen et al. (2011) examined high-NO_x isoprene SOA formed under high and low RH conditions and found that the high RH samples contained fewer oligomers than the low RH samples. Zhang et al. (2011) investigated the effect of RH on the composition of high-NO_x isoprene SOA and found that

15 oligoesters present in the SOA were suppressed at higher RH, while the formation of organosulfates was enhanced. Riva et al. (2016) studied the effect of RH on SOA made from oxidized isoprene hydroxy hydroperoxide (ISOPOOH) and found that increasing RH led to an increase in abundance of some oligomers while decreasing the abundance of other oligomers. Harvey et al. (2016) investigated the effect of RH on 3-hydroxypropanal ozonolysis SOA and found that increasing RH resulted in a decrease in SOA yield and a decrease in oligomerization.

20 The effect of RH on anthropogenic SOA, including SOA formed from toluene, m-xylene, and 1,3,5-trimethylbenzene (TMB) has been studied as well, however most of these studies focused on the effect of RH on the SOA yield (Zhou et al., 2011; Cocker III et al., 2001; Kamens et al., 2011; Cao and Jang, 2010). For instance, Cao et al. (2010) investigated the effect of RH on the yield of SOA made from toluene under both high and low-NO_x conditions and observed a negative correlation between RH and SOA yield for low-NO_x experiments, i.e., lower RH resulted in higher SOA yields. They also found no

25 significant RH dependence under high-NO_x conditions (Cao and Jang, 2010). However, White et al. (2014) investigated the effect of RH on composition of toluene SOA produced under high-NO_x conditions, and unlike Cao et al. (2010) observed slightly higher toluene SOA yields at elevated RH as well as higher yields of photooxidation products (White et al., 2014).

In this work, we have confirmed the results from Cao et al. (2010) that there is a significant negative correlation between RH and low-NO_x SOA from toluene SOA mass loading and observed a strong RH dependence on SOA molecular composition.

30 We attribute this effect to the more extensive oligomerization of SOA compounds driven by condensation reactions under dry conditions. These findings have important implications for toluene SOA concentrations in dry, urban areas, especially in areas where regulations aim to reduce NO_x emissions in the future.

2 Materials and Methods

SOA was generated by photooxidation of toluene under low-NO_x conditions in a 5 m^3 smog chamber surrounded by a bank of UV-B lights. Before each experiment, the chamber was humidified to the desired RH by flowing purified air (typical VOC mixing ratios below 1 ppb) through a Nafion humidifier (PermaPure). The temperature (±1 °C) and RH (±2% RH)

5   inside the chamber were monitored with a Vaisala HMT330 probe. No seed aerosol was used. Hydrogen peroxide (H_2O_2) was introduced to the chamber by injecting a measured volume of aqueous H_2O_2 (30 wt%) into a bulb where it was evaporated and carried into the chamber by a flow of purified air over a period of 30 minutes. In the high-NO_x experiments, gaseous NO (1000 ppm in N_2) was added to achieve a total NO concentration of 300 ppb (for the low-NO_x experiments this step was skipped). Next, toluene (Fisher Scientific, ACS grade) was introduced into the chamber in a similar manner, by

10   evaporating a measured volume of liquid toluene into a stream of air over a period of five minutes, which resulted in a toluene mixing ratio of 1000 ppb. Following the addition of gaseous reactants into the chamber, the UV lamps were turned on, photolyzing the H_2O_2 and resulting in a steady-state OH concentration of 1×10^6 molec·cm^{-3} (determined in a separate experiment). These high concentrations were chosen in order to produce a sufficient amount of SOA to collect for offline analysis. Throughout each experiment, particle concentrations were monitored with a Scanning Mobility Particle Sizer

15   (SMPS Model 3080, TSI Inc.).

SOA samples were collected onto Teflon filters for offline analysis by nano-DESI-HRMS. The SOA filter samples were analyzed in both positive and negative ion modes using an LTQ-Orbitrap mass spectrometer (Thermo Corp.) with a resolving power of 10^5 at m/z 400 equipped with a custom-built nano-DESI source (Roach et al., 2010a, b). Mass spectra of solvents and blank filters were recorded as controls. Mass spectra of related samples were clustered together, and the m/z

20   axis was calibrated internally with respect to known SOA products. The peaks were assigned formulas, $C_cH_hO_oN_nNa_{0-1}^+$ or $C_cH_hO_oN_n^-$, constrained by valence rules and elemental ratios (c,h,o,n refer to the number of corresponding atoms in the ion) (Kind and Fiehn, 2007). The resulting ion formulas were converted into formulas of the corresponding neutral species. All data reported below refers to the formula and molecular weights of the neutral species.

3 Results and Discussion

25   The raw mass spectra of a low RH sample (<2% RH) and a high RH sample (75% RH) are shown in Figure 1, plotted as a function of the molecular weight of the neutral compound. The mass spectra obtained in the positive and negative ion modes represent the SOA compounds ionizable in these modes, and are not expected to be identical (Walser et al., 2008). The low-NO_x mass spectrum shown in Figure 1 is qualitatively similar to the low-NO_x mass spectrum of toluene SOA discussed in a previous study which was prepared in a different smog chamber but analyzed by the same nano-DESI instrument (Lin et al.,

30   2015).

As shown in Figure 1, the increase in RH resulted in a visible reduction in the overall peak abundance for both ion modes, due to the fact that the high RH sample had a much lower particle mass during the SOA generation (see below), and thus

there was less material on the substrate. Despite this reduction in peak abundance, the major observed SOA compounds remained the same. Table 1 lists five most abundant peaks for both the low and high RH samples observed in positive and negative modes. The fact that the major peaks are so similar between the low and high RH samples suggests that the major products are produced by a similar mechanism that is not sensitive to RH.

5   While the major oxidation products were similar at low and high RH, the less abundant products were much more strongly affected by RH. Specifically, the abundances of high-molecular weight compounds were visibly reduced at high RH, suggesting that the oligomer formation is suppressed (Figure 1). To better quantify this effect, Figure 2 shows the combined peak abundances as a function of the number of carbon atoms in each molecule. Monomer compounds containing 7 carbon atoms and dimer compounds containing 14 carbon atoms clearly dominate the distribution. Many other compounds with

10   carbon numbers up to 32 also appear in the mass spectrum, and these minor compounds are the most affected by RH.

When comparing the low RH sample to the high RH sample, there is a significant decrease in combined peak abundance for molecules with more than 7 carbons under high RH conditions. This suggests that the abundance of dimers and trimers decreases with increasing RH. Because these higher molecular weight oligomers tend to have lower volatility (Li et al., 2016), they play an important role in the formation and growth of aerosol particles. With the lower fraction of oligomers

15   produced under high RH conditions, the population of the oxidation products becomes more volatile on average, which should result in a lower SOA yield such as those reported by Cao et al. (2010).

To better illustrate the possible effect of RH on the yield of condensable oxidation products, the volatility distributions were estimated for the low-NO$_x$ toluene SOA compounds using the "molecular corridor" approach (Li et al., 2016; Shiraiwa et al., 2014). This parameterization was developed specifically for atmospheric organic compounds containing oxygen, nitrogen,

20   and sulfur (Li et al., 2016), and it makes it possible to estimate the pure compound vapor pressure, C_0, from the elemental composition derived from high-resolution mass spectra (Lin et al., 2016; Romonosky et al., 2017). C_0 is related to the more commonly used effective saturation mass concentration, $C^* = \gamma \times C_0$, where γ is the activity coefficient (Pankow, 1994). C_0 becomes equal to C^* under the assumption of an ideal thermodynamic mixing. The C_0 values were calculated for each compound observed in the positive and negative ion mode mass spectra. The values were binned as commonly done in the

25   volatility basis set (VBS) (Donahue et al., 2006) in equally spaced bins of base-10 logarithm of C_0. The contribution of each compound to its volatility bin was taken to be proportional to its relative abundance in the mass spectrum. Because of the correlation between the ESI detection sensitivity and molecular weight (Nguyen et al., 2013), the mass fraction of the detected SOA compound can be taken to be proportional to its peak abundance. This is an approximation, but it may be suitable for comparing distributions for SOA produced and analyzed under the same experimental conditions (Romonosky et

30   al., 2017).

Figure 3 shows the resulting distribution of the SOA compounds by the volatility. Under typical ambient conditions, compounds with C_0 above ~10 µg m^{-3}, i.e., the ones falling above the log(C_0) =1 bin, should exist primarily in the gaseous phase. Some of these more volatile compounds were detected in the negative ion mode. They may correspond to carboxylic acids that adsorbed to the filter during sampling. Less volatile compounds were preferentially observed in the positive ion

mode. In both positive and negative ion modes, the compounds falling in the lower volatility bins were visibly suppressed at high RH. For example, the high RH to low RH ratio of the combined peak abundances for the compounds falling below $\log(C_0) = 1$ is 0.3 in the positive ion mode and 0.05 in the negative ion mode.

In order to investigate whether the decrease in oligomers affects the SOA mass loading, we have done additional
5 experiments in which the particle mass concentration was tracked with SMPS at different RH. The SMPS data were corrected for particle wall loss effects assuming an effective first-order rate constant for the loss of mass concentration of 9.3 $\times 10^{-4}$ min^{-1} measured in a separate experiment (the rate constant was assumed to be independent of particle size). Most of the SMPS experiments were performed under low-NO$_x$ conditions. However, in order to compare our results to the results of Cao et al. (2010), we did additional experiments under high-NO$_x$ conditions. A summary of these experiments is presented in
10 Table 2. Representative examples of the wall loss corrected particle mass concentration as a function of photooxidation reaction time are shown in Figure 4 for both the low-NO$_x$ and the high-NO$_x$ toluene SOA systems.

Under high-NO$_x$ conditions, there was a small difference in the maximum mass concentration achieved under <2%, 40%, and 75% RH (less than a factor of 2), but under low-NO$_x$ conditions the difference was substantially larger. For the low-NO$_x$ system, the wall loss corrected particle mass concentration decreased by a factor of 8 over the range of RHs studied. The
15 effect was reproducible as essentially the same mass concentration was observed in experiments repeated on different days under the same initial conditions.

The differences between the low and high RH systems cannot be explained by hygroscopic growth of particles at elevated RH. Throughout the experiment, the SMPS sampled air directly from the chamber. Each experiment lasted many hours, which allowed the sheath flow in the SMPS to approach the RH of the chamber air. Therefore, the particles sized by the
20 SMPS contained some aerosol liquid water and would appear larger than their dry size. If the organic mass in particles did not change at different RH levels, we would have observed an *increase* as opposed to a decrease in the measured particle mass concentration. With a typical hygroscopic growth factor (the ratio of particle diameters in the humidified and dry air) for SOA of 1.1 at 85% RH (Varutbangkul et al., 2006), the increase in the apparent mass concentration would have been by a factor of about 1.3. Instead, the mass concentration decreased by almost a factor of 8 at higher RHs. The strong dependence
25 of the low-NO$_x$ toluene SOA mass loading on RH is therefore not an artifact of the SMPS measurements. It is also consistent with results of Cao et al. (2010), who observed a negative correlation between RH and low-NO$_x$ toluene SOA yield, but no correlation between RH and high-NO$_x$ toluene SOA yield.

We cannot rule out the possibility that the mass loading of SOA was affected by the enhanced wall loss of more water soluble compounds under high RH conditions. It is conceivable that the products of low-NO$_x$ oxidation of toluene are more
30 soluble than the products of high-NO$_x$ oxidation of toluene. This would result a stronger effect of RH on the mass loading of low-NO$_x$ SOA. Distinguishing the wall-loss effects from the effect of water on the distribution of oligomers would require more careful chamber measurement of SOA yields over a broad range of concentrations and different and in the presence of seed aerosol (to suppress wall loss effects).

A possible chemical explanation for the observed RH effect is that there are chemical reactions in the system that directly involve water and change the chemical composition of the particles thereby affecting their growth rate. Previous studies have shown that RH can affect the composition and potential yield of SOA by altering the fraction of low-volatility oligomers in SOA. Increased RH could suppress oligomerization occurring by condensation reactions by shifting the reaction equilibrium

5   toward the products as discussed in Nguyen et al. (2011).

To investigate this possibility, we examined the frequency of occurrence of mass differences between the peaks in the high resolution mass spectra. Table 3 lists the most common mass differences in all four mass spectra. The most frequently observed mass difference in the low-RH sample was C_2H_2O, and its frequency of occurrence dropped in the high-RH sample. It is possible that C_2H_2O results from oligomerization chemistry of glycolaldehyde ($C_2H_4O_2$), which can react by

10   aldol condensation mechanism with compounds containing a carbonyl group (Scheme 1). Glycolaldehyde has been observed previously in oxidation of toluene (White et al., 2014; Yu et al., 1997), likely as an oxidation product of methylglyoxal. The difference corresponding to H_2O was not amongst the most common, however, it became more probable in the high RH sample, consistent with hydration reactions. Anhydrides, commonly found in toluene SOA (Bloss et al., 2005; Forstner et al., 1997), may undergo hydrolysis, which adds an H_2O unit to the formula.

15   We additionally tested whether oligomeric compounds occurring in low-RH toluene SOA can be produced by either simple addition or condensation of monomer compounds occurring in high-RH toluene SOA. If simple addition is responsible for the oligomerization, we would expect to see peaks in the low RH mass spectrum with molecular weights equal to the sum of two peaks from the high RH mass spectrum. If condensation is responsible for the oligomerization, we would expect to see peaks in the low RH mass spectrum with molecular weights equal to the sum of two peaks from the high RH mass spectrum

20   minus the mass of water. In positive ion mode, the fraction of peaks that could be matched by the addition reactions was 69%, while the fraction of peaks matched by the condensation reactions was 83%. These numbers were 62% and 69%, respectively, for negative ion mode. This suggests that condensation reactions (that remove water) are more likely to be responsible for the enhanced oligomer formation under dry conditions. This conclusion is similar to the one reached in the study of the effect of RH on oligomerization in high-NO_x isoprene SOA (Nguyen et al., 2011).

25   **4 Conclusions**

This study has demonstrated that the composition of low-NO_x toluene SOA depends on the RH under which it is produced. Oligomers produced by condensation reactions were observed in higher concentrations in the mass spectra of toluene SOA produced under low RH, and were suppressed under high RH conditions. Additionally, the mass loading of low-NO_x toluene SOA was reduced under high RH conditions. This is consistent with the results of Cao et al. (2010) who also reported a

30   negative correlation between RH and toluene SOA yield. This correlation was much weaker for high-NO_x toluene SOA in this study and was not observed by Cao et al. (2010). The plausible reason for the suppression of SOA mass loading at high RH is the change in the SOA chemical composition that favors lower-molecular weight, more volatile compounds. The

reduction of dimers and trimers in the high RH samples suggests that low volatility oligomers are not forming in toluene SOA under low-NO_x conditions, which means particle growth is suppressed and mass loading is reduced.

These results have potential impacts in the urban atmospheric environment where toluene is commonly present alongside NO_x because both are emitted by anthropogenic sources. Under high-NO_x conditions, the total amount of toluene SOA will not depend strongly on atmospheric RH. However, these results suggest that if NO_x in urban areas is significantly reduced, the total amount of toluene SOA would be similarly suppressed under normal atmospheric conditions (~50% RH), even if toluene emissions stay the same. This may be relevant in cities like Los Angeles, which plan to significantly reduce NO_x emissions in the atmosphere.

Additionally, there are many locations that become dry under certain meteorological conditions. For example, during California's Santa Ana winds, the RH regularly decreases below 10%. Under such dry atmospheric conditions in a low-NO_x environment, the yield of toluene SOA would no longer be suppressed. This change would result in a "burst" of toluene SOA, changing the overall concentration of SOA in the area.

It is also conceivable that the effect of RH on the SOA yield is a common feature of all low-NO_x aromatic SOA, all of which should contain aldehyde compounds capable of oligomerization by condensation reactions. If this is the case, the production of SOA from naturally emitted aromatic compounds (indole, benzyl acetate, benzaldehyde, etc.), which exist in low-NO_x environments, would be strongly modulated by the ambient relative humidity.

Acknowledgements

This research was enabled by funding from the United States Environmental Protection Agency under grant EPA 83588101. Julia Montoya acknowledges support from the California LSAMP Bridge to the Doctorate Program at the University of California, Irvine, which is funded by grant NSF-1500284. The PTR-ToF-MS instruments used in this work was purchased with grant NSF MRI-0923323. The HRMS measurements were performed at the W.R. Wiley Environmental Molecular Sciences Laboratory (EMSL) – a national scientific user facility located at PNNL, and sponsored by the Office of Biological and Environmental Research of the U.S. DOE. PNNL is operated for U.S. DOE by Battelle Memorial Institute under Contract No. DE-AC06-76RL0 1830.

References

Bateman, A. P., Nizkorodov, S. A., Laskin, J., and Laskin, A.: Photolytic processing of secondary organic aerosols dissolved in cloud droplets, Phys. Chem. Chem. Phys., 13, 12199-12212, 10.1039/c1cp20526a, 2011.
Bloss, C., Wagner, V., Jenkin, M. E., Volkamer, R., Bloss, W. J., Lee, J. D., Heard, D. E., Wirtz, K., Martin-Reviejo, M., Rea, G., Wenger, J. C., and Pilling, M. J.: Development of a detailed chemical mechanism (MCMv3.1) for the atmospheric oxidation of aromatic hydrocarbons, Atmos. Chem. Phys., 5, 641-664, 10.5194/acp-5-641-2005, 2005.

Cao, G., and Jang, M.: An SOA Model for Toluene Oxidation in the Presence of Inorganic Aerosols, Environmental Science & Technology, 44, 727-733, 10.1021/es901682r, 2010.

Cocker III, D. R., Clegg, S. L., Flagan, R. C., and Seinfeld, J. H.: The effect of water on gas–particle partitioning of secondary organic aerosol. Part I: α-pinene/ozone system, Atmospheric Environment, 35, 6049-6072,
5   http://dx.doi.org/10.1016/S1352-2310(01)00404-6, 2001.

Donahue, N. M., Robinson, A. L., Stanier, C. O., and Pandis, S. N.: Coupled Partitioning, Dilution, and Chemical Aging of Semivolatile Organics, Environmental Science & Technology, 40, 2635-2643, 10.1021/es052297c, 2006.

Ervens, B., Turpin, B. J., and Weber, R. J.: Secondary organic aerosol formation in cloud droplets and aqueous particles (aqSOA): a review of laboratory, field and model studies, Atmos. Chem. Phys., 11, 11069-11102, 10.5194/acp-11-11069-
10   2011, 2011.

Finlayson-Pitts, B. J., and Pitts Jr, J. N.: Chapter 6 - Rates and Mechanisms of Gas-Phase Reactions in Irradiated Organic −NOx—Air Mixtures, in: Chemistry of the Upper and Lower Atmosphere, Academic Press, San Diego, 179-263, 2000.

Forstner, H. J. L., Flagan, R. C., and Seinfeld, J. H.: Secondary Organic Aerosol from the Photooxidation of Aromatic Hydrocarbons: Molecular Composition, Environmental Science & Technology, 31, 1345-1358, 10.1021/es9605376, 1997.

15   Harvey, R. M., Bateman, A. P., Jain, S., Li, Y. J., Martin, S., and Petrucci, G. A.: Optical Properties of Secondary Organic Aerosol from cis-3-Hexenol and cis-3-Hexenyl Acetate: Effect of Chemical Composition, Humidity, and Phase, Environmental Science & Technology, 50, 4997-5006, 10.1021/acs.est.6b00625, 2016.

Herrmann, H., Schaefer, T., Tilgner, A., Styler, S. A., Weller, C., Teich, M., and Otto, T.: Tropospheric Aqueous-Phase Chemistry: Kinetics, Mechanisms, and Its Coupling to a Changing Gas Phase, Chemical Reviews, 115, 4259-4334,
20   10.1021/cr500447k, 2015.

Jang, M., Czoschke, N. M., Lee, S., and Kamens, R. M.: Heterogeneous Atmospheric Aerosol Production by Acid-Catalyzed Particle-Phase Reactions, Science, 298, 814-817, 10.1126/science.1075798, 2002.

Kamens, R. M., Zhang, H., Chen, E. H., Zhou, Y., Parikh, H. M., Wilson, R. L., Galloway, K. E., and Rosen, E. P.: Secondary organic aerosol formation from toluene in an atmospheric hydrocarbon mixture: Water and particle seed effects,
25   Atmospheric Environment, 45, 2324-2334, http://dx.doi.org/10.1016/j.atmosenv.2010.11.007, 2011.

Kind, T., and Fiehn, O.: Seven Golden Rules for heuristic filtering of molecular formulas obtained by accurate mass spectrometry, BMC Bioinformatics, 8, 105-105, 10.1186/1471-2105-8-105, 2007.

Li, Y., Pöschl, U., and Shiraiwa, M.: Molecular corridors and parameterizations of volatility in the chemical evolution of organic aerosols, Atmos. Chem. Phys., 16, 3327-3344, 10.5194/acp-16-3327-2016, 2016.

30   Lin, P., Liu, J., Shilling, J. E., Kathmann, S., Laskin, J., and Laskin, A.: Molecular Characterization of Brown Carbon (BrC) Chromophores in Secondary Organic Aerosol Generated From Photo-Oxidation of Toluene, Physical Chemistry Chemical Physics, 23312-23325 10.1039/C5CP02563J, 2015.

Lin, P., Aiona, P. K., Li, Y., Shiraiwa, M., Laskin, J., Nizkorodov, S. A., and Laskin, A.: Molecular Characterization of Brown Carbon in Biomass Burning Aerosol Particles, Environmental Science & Technology, 50, 11815-11824,
35   10.1021/acs.est.6b03024, 2016.

Nguyen, T. B., Roach, P. J., Laskin, J., Laskin, A., and Nizkorodov, S. A.: Effect of humidity on the composition of isoprene photooxidation secondary organic aerosol, Atmos. Chem. Phys., 11, 6931-6944, 10.5194/acp-11-6931-2011, 2011.

Nguyen, T. B., Lee, P. B., Updyke, K. M., Bones, D. L., Laskin, J., Laskin, A., and Nizkorodov, S. A.: Formation of nitrogen- and sulfur-containing light-absorbing compounds accelerated by evaporation of water from secondary organic
40   aerosols, Journal of Geophysical Research: Atmospheres, 117, D01207, 10.1029/2011JD016944, 2012.

Nguyen, T. B., Laskin, A., Laskin, J., and Nizkorodov, S. A.: Brown carbon formation from ketoaldehydes of biogenic monoterpenes, Faraday Discuss., 165, 473-494, 10.1039/c3fd00036b, 2013.

Pankow, J. F.: An absorption model of gas/particle partitioning of organic compounds in the atmosphere, Atmospheric Environment, 28, 185-188, http://dx.doi.org/10.1016/1352-2310(94)90093-0, 1994.

45   Perraud, V., Bruns, E. A., Ezell, M. J., Johnson, S. N., Yu, Y., Alexander, M. L., Zelenyuk, A., Imre, D., Chang, W. L., Dabdub, D., Pankow, J. F., and Finlayson-Pitts, B. J.: Nonequilibrium atmospheric secondary organic aerosol formation and growth, Proceedings of the National Academy of Sciences, 2836-2841, 10.1073/pnas.1119909109, 2012.

Renbaum-Wolff, L., Grayson, J. W., Bateman, A. P., Kuwata, M., Sellier, M., Murray, B. J., Shilling, J. E., Martin, S. T., and Bertram, A. K.: Viscosity of α-pinene secondary organic material and implications for particle growth and reactivity,
50   Proc. Natl. Acad. Sci. U. S. A., 110, 8014-8019, 10.1073/pnas.1219548110, 2013.

Riva, M., Budisulistiorini, S. H., Chen, Y., Zhang, Z., D'Ambro, E. L., Zhang, X., Gold, A., Turpin, B. J., Thornton, J. A., Canagaratna, M. R., and Surratt, J. D.: Chemical Characterization of Secondary Organic Aerosol from Oxidation of Isoprene Hydroxyhydroperoxides, Environmental Science & Technology, 9889–9899, 10.1021/acs.est.6b02511, 2016.

5 Roach, P. J., Laskin, J., and Laskin, A.: Molecular Characterization of Organic Aerosols Using Nanospray-Desorption/Electrospray Ionization-Mass Spectrometry, Analytical Chemistry, 82, 7979-7986, 10.1021/ac101449p, 2010a.

Roach, P. J., Laskin, J., and Laskin, A.: Nanospray desorption electrospray ionization: an ambient method for liquid-extraction surface sampling in mass spectrometry, Analyst, 135, 2233-2236, 10.1039/C0AN00312C, 2010b.

Romonosky, D. E., Laskin, A., Laskin, J., and Nizkorodov, S. A.: High-Resolution Mass Spectrometry and Molecular Characterization of Aqueous Photochemistry Products of Common Types of Secondary Organic Aerosols, The Journal of
10 Physical Chemistry A, 119, 2594-2606, 10.1021/jp509476r, 2015.

Romonosky, D. E., Li, Y., Shiraiwa, M., Laskin, A., Laskin, J., and Nizkorodov, S. A.: Aqueous Photochemistry of Secondary Organic Aerosol of α-Pinene and α-Humulene Oxidized with Ozone, Hydroxyl Radical, and Nitrate Radical, The Journal of Physical Chemistry A, 1298–1309, 10.1021/acs.jpca.6b10900, 2017.

Seinfeld, J. H., and Pandis, S. N.: Atmospheric Chemistry and Physics: From Air Pollution to Climate Change, Wiley, 2016.
15 Shiraiwa, M., and Seinfeld, J. H.: Equilibration timescale of atmospheric secondary organic aerosol partitioning, Geophysical Research Letters, 39, L24801, 10.1029/2012GL054008, 2012.

Shiraiwa, M., Berkemeier, T., Schilling-Fahnestock, K. A., Seinfeld, J. H., and Pöschl, U.: Molecular corridors and kinetic regimes in the multiphase chemical evolution of secondary organic aerosol, Atmos. Chem. Phys., 14, 8323-8341, 10.5194/acp-14-8323-2014, 2014.

20 Varutbangkul, V., Brechtel, F. J., Bahreini, R., Ng, N. L., Keywood, M. D., Kroll, J. H., Flagan, R. C., Seinfeld, J. H., Lee, A., and Goldstein, A. H.: Hygroscopicity of secondary organic aerosols formed by oxidation of cycloalkenes, monoterpenes, sesquiterpenes, and related compounds, Atmos. Chem. Phys., 6, 2367-2388, 10.5194/acp-6-2367-2006, 2006.

Walser, M. L., Desyaterik, Y., Laskin, J., Laskin, A., and Nizkorodov, S. A.: High-resolution mass spectrometric analysis of secondary organic aerosol produced by ozonation of limonene, Physical Chemistry Chemical Physics, 10, 1009-1022,
25 10.1039/B712620D, 2008.

White, S. J., Jamie, I. M., and Angove, D. E.: Chemical characterisation of semi-volatile and aerosol compounds from the photooxidation of toluene and NOx, Atmospheric Environment, 83, 237-244, http://dx.doi.org/10.1016/j.atmosenv.2013.11.023, 2014.

Yu, J., Jeffries, H. E., and Sexton, K. G.: Atmospheric photooxidation of alkylbenzenes—I. Carbonyl product analyses,
30 Atmospheric Environment, 31, 2261-2280, http://dx.doi.org/10.1016/S1352-2310(97)00011-3, 1997.

Zhang, H., Surratt, J. D., Lin, Y. H., Bapat, J., and Kamens, R. M.: Effect of relative humidity on SOA formation from isoprene/NO photooxidation: enhancement of 2-methylglyceric acid and its corresponding oligoesters under dry conditions, Atmos. Chem. Phys., 11, 6411-6424, 10.5194/acp-11-6411-2011, 2011.

Zhou, Y., Zhang, H., Parikh, H. M., Chen, E. H., Rattanavaraha, W., Rosen, E. P., Wang, W., and Kamens, R. M.:
35 Secondary organic aerosol formation from xylenes and mixtures of toluene and xylenes in an atmospheric urban hydrocarbon mixture: Water and particle seed effects (II), Atmospheric Environment, 45, 3882-3890, http://dx.doi.org/10.1016/j.atmosenv.2010.12.048, 2011.
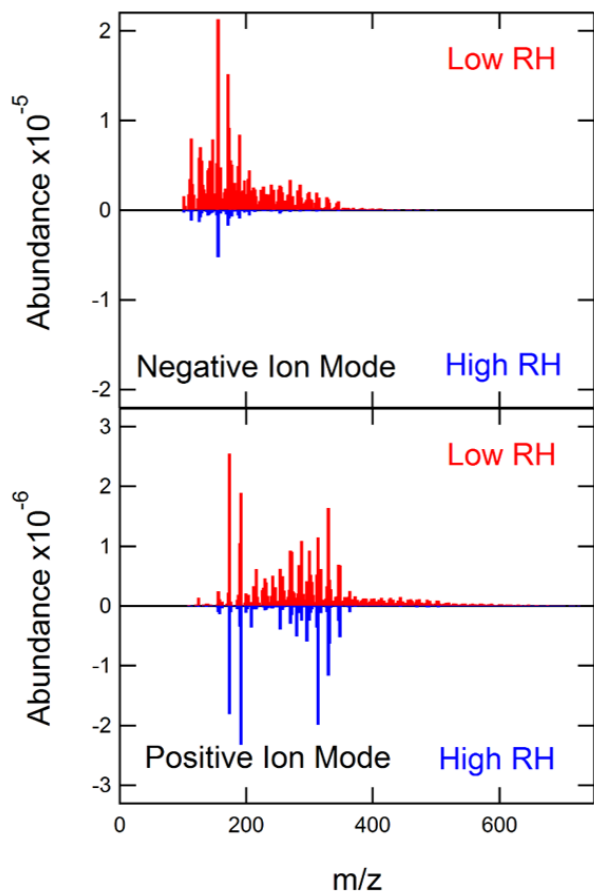
Figure 1: High-resolution mass spectra obtained in negative ion mode (top) and positive ion mode (bottom). The red upward-pointing mass spectra represent the sample made under low RH (<2%) and the blue inverted mass spectra represent the sample made under high RH (75%).

Table 1: Five most abundant compounds observed in the low and high RH low-NO$_x$ toluene SOA samples. In negative ion mode, the same most abundant peaks were observed at the low and high RH. In positive ion mode, the most abundant species differed by one compound in the low and high RH experiments, hence the table contains 6 formulas.

Positive Ion Mode		Normalized Peak Abundance	
Nominal Mass	Formula	Low RH	High RH
174	$C_7H_{10}O_5$	1	1
192	$C_7H_{12}O_6$	0.74	0.86
330	$C_{14}H_{18}O_9$	0.64	0.78
314	$C_{14}H_{18}O_8$	0.45	0.50
288	$C_{12}H_{16}O_8$	0.43	0.11
332	$C_{14}H_{20}O_9$	0.17	0.27
Negative Ion Mode		Normalized Peak Abundance	
Nominal Mass	Formula	Low RH	High RH
156	$C_7H_8O_4$	1	1
172	$C_7H_8O_5$	0.71	0.86
174	$C_7H_{10}O_5$	0.43	0.78
190	$C_7H_{10}O_6$	0.40	0.50
114	$C_5H_6O_3$	0.38	0.27
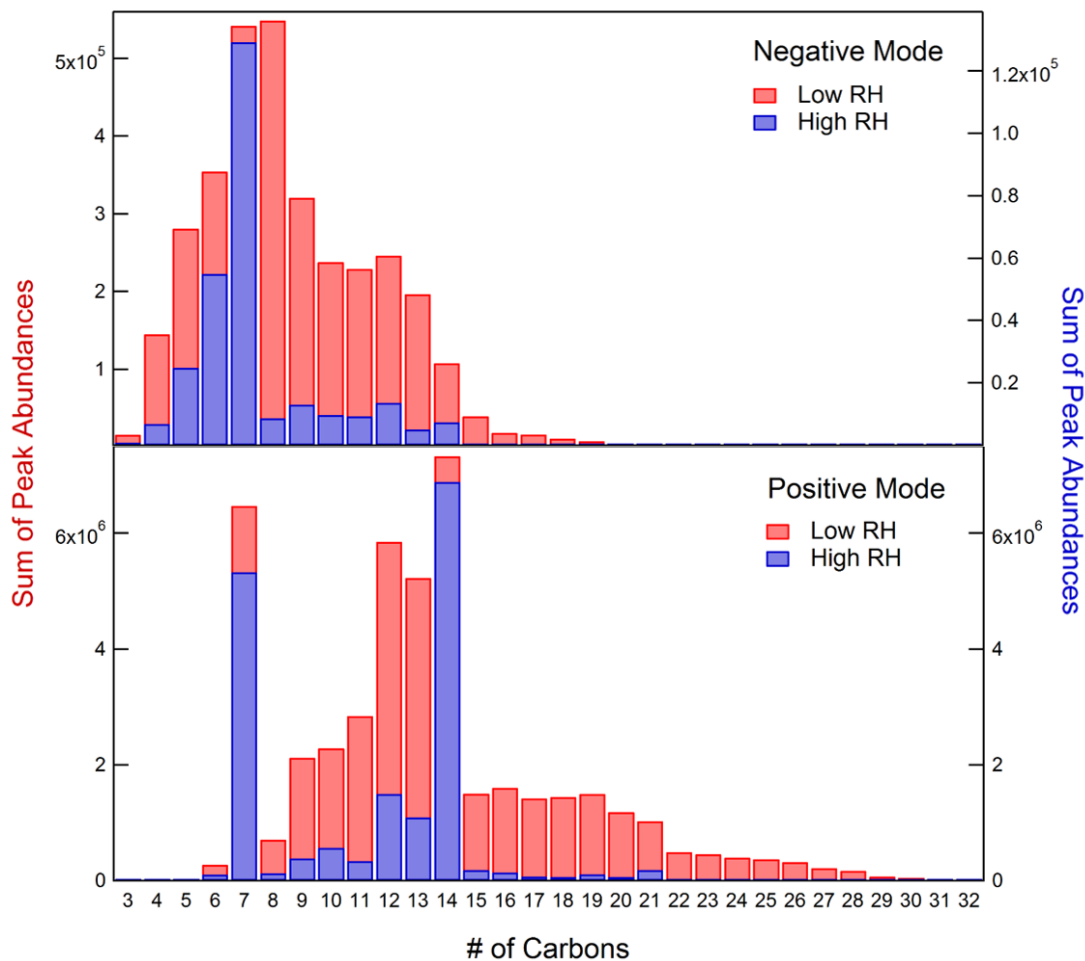
Figure 2: Combined abundance of all peaks as a function of number of carbon atoms in negative mode (top) and positive mode (bottom). The data for the low RH sample are shown in red and the data for the high RH sample are shown in blue.
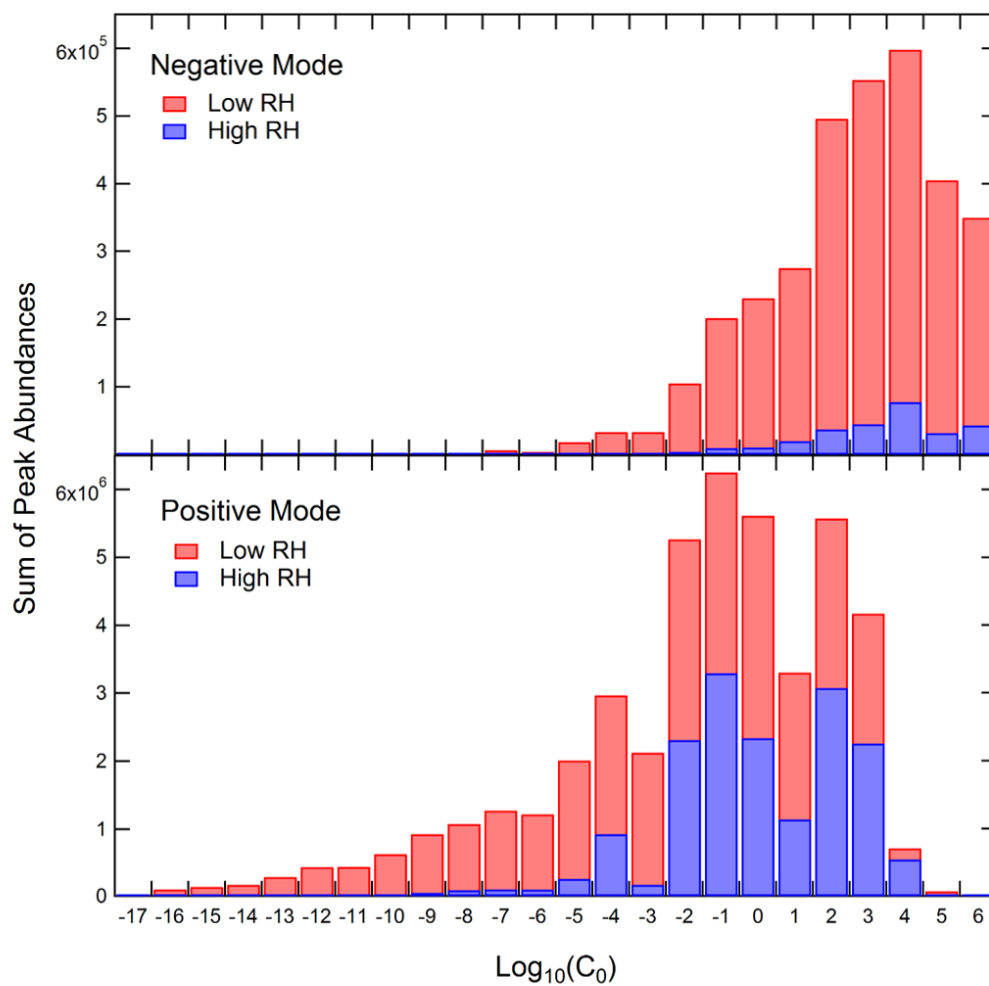
Figure 3. Estimated volatility distribution for the compounds observed in the positive (a) and negative (b) ion mode at high (red bars) and low (blue bars) RH. The height of each bar is proportional to the total ESI abundance of compounds falling within the volatility bin.

Table 2: Summary of SMPS experiments. The uncertainties included in this table are based on the standard deviation in the data.

Initial RH	# of Experiments	NO_x ppm	Toluene ppm	H_2O_2 ppm	SOA from SMPS $\mu g/m^3$	Wall Loss Corrected SOA $\mu g/m^3$
Low-NO_x – High Toluene						
<2	4	-	1.0	2.0	180 ± 20	210 ± 20
20 ± 3	2	-	1.0	2.0	76 ± 4	87 ± 6
43	1	-	1.0	2.0	74	84
76 ± 1	4	-	1.0	2.0	27 ± 7	28 ± 7
89 ± 1	2	-	1.0	2.0	25 ± 8	26 ± 9
Low-NO_x – Lower Toluene						
<2	1	-	0.3	0.6	23	27
75	1	-	0.3	0.6	8	9
High-NO_x – High Toluene						
<2	1	0.3	1.0	2.0	330	390
43	1	0.3	1.0	2.0	210	260
77	1	0.3	1.0	2.0	230	270
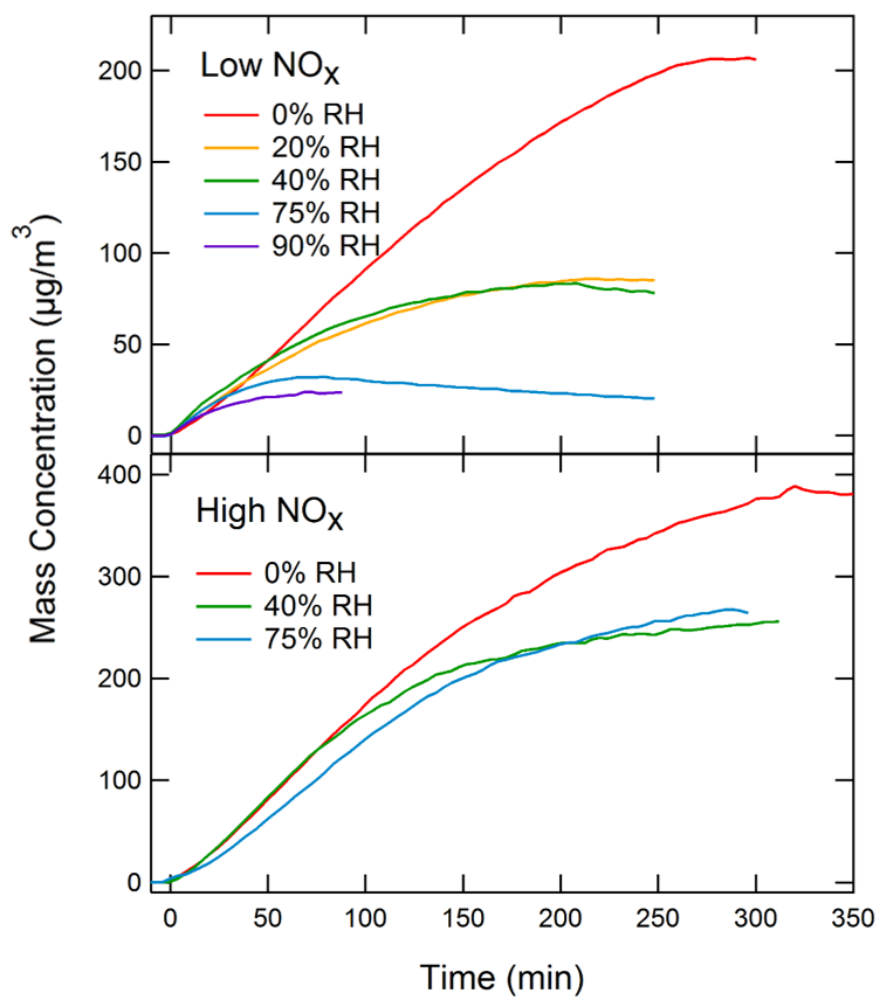
Figure 4: Examples of particle mass concentration measurements by SMPS (corrected for wall-loss) as a function of photooxidation time under low-NOx (top) and high-NOx (bottom) conditions.
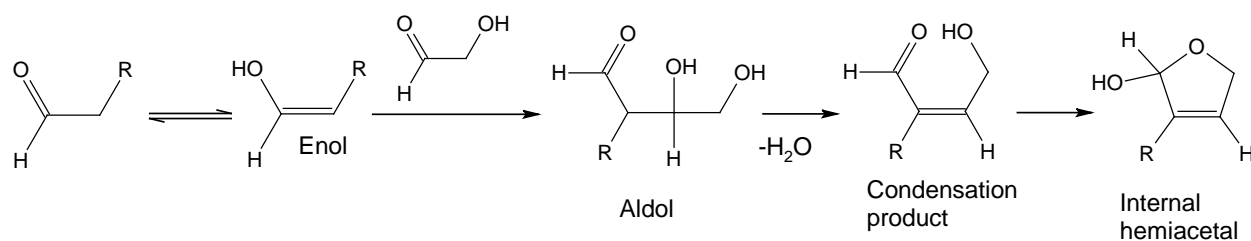
Scheme 1: An aldol condensation reaction involving glycolaldehyde that results in an addition of C₂H₂O to the formula of the
5   **aldehyde co-reactant.**

Table 3: Most common mass differences in the high resolution mass spectra of low-NO$_x$ toluene SOA (in the order of decreasing
10 **frequency of occurrence).**

Positive Ion Mode		Negative Ion Mode	
Low RH	**High RH**	**Low RH**	**High RH**
C_2H_2O	CH_2	C	O
CH_2O	O	C_2H_2O	CH_2O
C	CH_2O	O	C
CH_2	C_2H_2O	CH_2O	C_2H_2O
O	C	CH_2	CH_2
$C_3H_4O_2$	CO	CO	C_2H_2